Structure of the Stress Response Protein DR1199 from *Deinococcus radiodurans*: A Member of the DJ-1 Superfamily

Emanuela Fioravanti,[‡] M. Asunción Durá,[§] David Lascoux,[||] Elena Micossi,[‡] Bruno Franzetti,[§] and Sean McSweeney*[,‡]

European Synchrotron Radiation Facility, BP 220, 38043 Grenoble Cedex 9, France, and Laboratoire de Biophysique Moléculaire and Laboratoire de Spectrométrie de Masse des Protéines, Institut de Biologie Structurale J.-P. Ebel CEA CNRS UJF, 41 Rue Jules Horowitz, 38027 Grenoble Cedex 1, France

Received May 13, 2008; Revised Manuscript Received September 4, 2008

ABSTRACT: The expression level of protein DR1199 is observed to increase considerably in the radioresistant bacterium *Deinococcus radiodurans* following irradiation. This protein belongs to the DJ-1 superfamily, which includes proteins with diverse functions, such as the archaeal proteases *Ph*pI and *Pf*pI, the bacterial chaperone Hsp31 and hyperosmotic stress protein YhbO, and the human Parkinson's disease-related protein DJ-1. All members of the superfamily are oligomeric, and the oligomerization interface varies from protein to protein. Although for many of these proteins, their function remains obscure, most of them are involved in cellular protection against environmental stresses. We have determined the structure of DR1199 to a resolution of 2.15 Å, and we have tested its function and studied its role in the response to irradiation and more generally to oxidative stress in *D. radiodurans*. The protein is a dimer displaying an oligomerization interface similar to that observed for the YhbO and *Ph*pI proteins. The cysteine in the catalytic triad (Cys 115) is oxidized in our structure, similar to modifications seen in the corresponding cysteine of the DJ-1 protein. The oxidation occurs spontaneously in DR1199 crystals. In solution, no proteolytic or chaperone activity was detected. On the basis of our results, we suggest that DR1199 might work as a general stress protein involved in the detoxification of the cell from oxygen reactive species, rather than as a peptidase in *D. radiodurans*.

Deinococcus radiodurans is a nonpathogenic, Gram-positive bacterium that can survive exposure to doses of ionizing radiation that are lethal to virtually all other organisms. This outstanding resistance has been attributed to a number of factors, including an enhanced repair system that provides exceptional protection and stability of the *D. radiodurans* genome (*1*−*3*), the accumulation of Mn(II) responsible for the detoxification of oxygen reactive species and protection of the bacterial proteins from oxidation (*4, 5*), and an unusually high number of predicted highly expressed genes (*6*), encoding detoxification proteins whose levels of expression significantly increase after irradiation of the cells (*7*).

The gene of DR1199 [also known as Protease I (*8*)] is predicted to be highly expressed (*6*), and indeed, its expression level is observed to increase following different types of stress in *D. radiodurans*, including γ-irradiation (*7*), heat shock (*9*), and X-ray irradiation (this study). DR1199 is a member of the DJ-1/ThiJ/*Pf*pI superfamily (DJ-1 hereafter), which includes proteins spanning many functions, including acting as chaperones, proteases, catalases, general stress response proteins, enzymes involved in thiamine biosynthesis, and the DJ-1 protein, which is mutated in autosomal recessive early onset Parkinson's disease (*10*).

Although the function of many members of the DJ-1 superfamily remains unknown, those that have been characterized are mostly involved in the cell response to stress. *Escherichia coli* Hsp31 is involved in thermal stress protection and acid resistance (*11, 12*), human DJ-1 in cellular protection against oxidative stress (*13*), and *E. coli* YhbO in the response to hyperosmotic or acid stress (*14*). A YhbO-disrupted mutant of *E. coli* is highly sensitive to oxidative, thermal, UV, and pH stresses (*15*).

All members of the DJ-1 superfamily are oligomers. While the oligomeric state of these proteins appears to be crucial either to their stability or to their biochemical activity, it varies widely, ranging from dimers to dodecamers with the oligomerization interface differing among the family members (*16*−*18*).

All the protein structures available for this superfamily contain a similar domain characterized by a sharp turn between a β-strand and an α-helix, the "nucleophile elbow" (*19*), carrying an important cysteine. This residue is part of the proposed Cys, His, Glu/Asp catalytic triad responsible for the peptidase activities of the *E. coli* Hsp31 chaperone (*20*) and the *Pyrococcus furiosus* (*21*) and *Pyrococcus horikoshii* (*22*) protease I (*Pf*pI and *Ph*pI[1], respectively).

*Ph*pI and *Pf*pI belong to a subgroup of the DJ-1 superfamily, class III of the Hsp31 family. Proteins in the Hsp31 family are divided into three classes on the basis of their

* To whom correspondence should be addressed. Telephone: 33 (0)4 76 88 23 62. Fax: 33 (0)4 76 88 21 60. E-mail: mcsweeney@esrf.fr.
[‡] European Synchrotron Radiation Facility.
[§] Laboratoire de Biophysique Moléculaire, Institut de Biologie Structurale J.-P. Ebel CEA CNRS UJF.
[||] Laboratoire de Spectrométrie de Masse des Protéines, Institut de Biologie Structurale J.-P. Ebel CEA CNRS UJF.

10.1021/bi800882v CCC: $40.75
Published on Web 10/14/2008

superstructure. Members of class I contain an "A" domain plus an extra smaller domain called the "P" domain; class II members have the A domain and an incomplete P domain, and class III proteins have only the A domain (*20*). These three classes also display differences in their active sites where the triad is formed by Cys, His, and Asp for class I and Cys, His, and Glu for classes II and III. *Pf*pI has been biochemically characterized (*21*), and the structure of *Ph*pI is available [*22*; Protein Data Bank (PDB) entry 1G2I]. Both proteins show proteolytic activity and can be isolated as dimers, trimers, and hexamers. *Pf*pI and *Ph*pI are classified as members of the C56 family of peptidases. DR1199 is classified in the MEROPS peptidase database [http://merops.sanger.ac.uk (*23*)] as a non-peptidase homologue of the same family.

We found that the expression level of DR1199 increases considerably after exposure of *D. radiodurans* cells to synchrotron radiation and decided to investigate the role of this protein in the protection and recovery from irradiation and oxidative stress in the bacterium. For this purpose, we determined the structure and studied the function of the protein.

MATERIALS AND METHODS

Protein Expression and Purification. The gene encoding DR1199, including an N-terminal His tag and a TEV-protease cleavage site, was cloned by the Molecular Biology and Protein Expression Automated Platform (RoBioMol, http://www.ibs.fr/content/ibs_eng/presentation/Platform/RobioMol) at the Institut de Biologie Structurale (Grenoble, France). The *E. coli* BL21(DE3)* expression strain was transformed with the vector containing the gene of interest using heat shock. A resulting transformant was used in large-scale expression in 3 L of LB medium containing 100 mg/mL ampicillin. The cells were grown by being vigorously shaken at 310 K until the optical density at 600 nm (OD_{600}) reached 0.6, and expression was induced by adding 0.5 mM isopropyl β-D-thiogalactopyranoside (IPTG). The cells were harvested 3 h postinduction by centrifugation at 5000*g* for 30 min and then resuspended in lysis buffer [50 mM Tris-HCl (pH 7.5), 150 mM NaCl, and 1 mM $MgCl_2$]; proteinase inhibitors (Roche), DNase I (Sigma-Aldrich), and lysozyme (Sigma-Aldrich) were added, and the cells were disrupted using a cell disruptor (Stansted Fluid Power Ltd.). The recombinant protein was isolated from the cell debris by centrifugation at 21000*g* for 30 min. The resulting protein extract was loaded onto a 5 mL HisTrap HP nickel chelating column (GE Healthcare) equilibrated with buffer A [50 mM Tris-HCl (pH 7.5) and 150 mM NaCl]. The protein was eluted using a gradient from 0 to 100% buffer B [50 mM Tris-HCl (pH 7.5), 150 mM NaCl, and 500 mM imidazole]. The protein was dialyzed overnight against buffer A to eliminate the imidazole from the preparation, then concentrated to 10 mg/mL, and stored at 193 K. Part of the protein preparation containing the N-terminal His tag and the TEV-protease cleavage site was used for crystallization. The rest of the preparation was incubated at 4 °C overnight with TEV-protease to remove the His tag. A DR1199:TEV-protease ratio of 5:1 was used in buffer A, added with 0.5 mM EDTA and 1 mM DTT. The cleaved DR1199 was then loaded for a second time onto a 5 mL nickel column, and the flow-through fractions were collected. The cleaved protein sequence contains residues 1−199 plus one additional N-terminal glycine. Coomassie-stained SDS−PAGE showed that the eluted protein was relatively pure. The protein was subsequently concentrated to 7 mg/mL, stored at 193 K, and used for crystallization, activity tests, and analysis by mass spectrometry.

Irradiation Experiments and Proteome Analysis. D. radiodurans cells were grown in 240 mL of liquid medium 53 at 30 °C. When the concentration reached midlog phase ($OD_{600} = 1$), the cells were separated in two batches: the control sample (nonirradiated) and the sample to be irradiated. Cells were concentrated to a volume of 2 mL and irradiated with X-rays on medical beamline ID17 at the ESRF, using a white beam (spectrum range of 50−300 keV, beam size of 0.5 cm × 1.2 cm). Cells were kept at 4 °C during irradiation. A dose rate of 17200 Gy/s was used, to a total absorbed dose of 5000 Gy. After irradiation, the cells were resuspended to their original volume in fresh medium and samples collected at different recovery times (5 min, 30 min, 1 h, 3 h, 6 h, and 12 h). The proteins were chemically extracted in 7 M urea, 7 M thiourea, 4% CHAPS, 40 mM DTT, 20 mM spermine, and Tris/EDTA/sucrose and separated on two-dimensional (2D) PAGE gels. 2D PAGE gels were run with an Ettan DIGE system using CyDye fluors fluorescent tags (Amersham Bioscience). The gels were analyzed using Image Master 2D Platinum (GE Healthcare); proteins for which an increase of more than 3-fold was observed were identified by mass spectrometry.

Protein Crystallization and Data Collection. The best crystals of DR1199 were obtained by the hanging drop vapor diffusion method using the uncleaved protein (N-terminal His tag and the TEV-protease cleavage site present in the polypeptide chain). Each drop was prepared by mixing 2 μL of a DR1199 protein solution with an equal volume of reservoir solution [0.2 M magnesium formate (pH 5.9) and 20% (w/v) PEG 3350]. The drops were equilibrated against 0.5 mL of this reservoir solution, and crystals grew in ~2 months to a nominal size of ca. 150 μm × 100 μm × 100 μm. The crystal used to determine the DR1199 structure was transferred to a cryoprotectant solution [0.2 M magnesium formate (pH 5.9), 20% (w/v) PEG 3350, and 20% glycerol] for 2 min prior to being flash-cooled in gaseous nitrogen for data collection. Diffraction data were collected at 100 K on beamline ID14-2 at the European Synchrotron Radiation Facility and processed with MOSFLM (*24*). Further data analysis was carried out using the CCP4 suite (*25*). Data collection statistics are summarized in Table 1.

Structure Determination and Refinement. DR1199 crystals belong to space group $P2_12_12$ with the following cell dimensions: $a = 65.8$ Å, $b = 88.6$ Å, and $c = 64.1$ Å. The asymmetric unit accommodates the native dimer with a solvent content of 38% (v/v). The structure of DR1199 was determined by molecular replacement with PHASER (*26*) using an N-terminally truncated C_α model of the *E. coli* YhbO protein (PDB entry 1OI4) that is 38% identical in sequence to DR1199. A starting partial model was obtained by automatic model building with ARP/wARP (*27*). The

[1] Abbreviations: *Ph*pI and *Pf*pI, *Pyrococcus horikoshii* and *Pyrococcus furiosus* protease I, respectively; TLS, translation-libration-screw; DLS, dynamic light scattering; FITC, fluorescein-isothiocyanate; AMC, 7-aminomethylcoumarin; pNA, *p*-nitroaniline; CS, citrate synthase.

Table 1: Data Collection and Refinement Statistics[a]

beamline	ID14-2
space group	$P2_12_12$
unit cell (Å)	$a = 65.8$
	$b = 88.6$
	$c = 64.1$
resolution (Å) (highest bin)	20−2.15 (2.27−2.15)
wavelength (Å)	0.933
no. of unique reflections	20998 (3015)
multiplicity	6.9 (6.8)
completeness (%)	99.8 (99.9)
mean I/σ_I	20.5 (3.0)
R_{sym}[b] (%)	7.5 (51.9)
R_{cryst}[c] (R_{free}[d]) (%)	20.0 (26.1)
rmsd[e] for bond lengths (Å)	0.011
rmsd[e] for bond angles (deg)	1.313
mean B[f] (Å^2)	22.3

[a] Numbers in parentheses refer to the highest-resolution shell. [b] $R_{sym} = \sum|I_{obs} - \langle I\rangle|/\sum\langle I\rangle$. [c] $R_{cryst} = \sum|F_{obs} - F_{calc}|/\sum F_{obs}$. [d] R_{free} was calculated with a small fraction (5%) of randomly selected reflections. [e] rmsd, root-mean-square deviation. [f] B, average isotropic temperature factor. Residual B factor only (not including the contribution from the TLS parameters).

initial model was then manually completed using COOT (*28*). Refinement using REFMAC (*29*) and further cycles of manual model building using COOT gave the final model consisting of 185 residues for each monomer. In both monomers, the electron density is so poor for the region including the His tag and the TEV-protease cleavage site that no model could be built for ~20 N-terminal residues, this problem being likely due to disorder associated with this unstructured part of the protein. The structure was refined using bulk solvent correction and a maximum-likelihood target function. The final cycles included translation-libration-screw (TLS) refinement of anisotropic displacement parameters (*30*) and were performed with REFMAC5 (*31*) in the CCP4 suite of programs. All the data measured, excluding a 5% test set for the calculation of R_{free}, were used in the refinement. The side chain atoms without visible electron density at 1.0σ were removed from the model. The quality of the structures was assessed using PROCHECK (*32*) and WHAT IF (*33*). Refinement statistics and geometry analysis of the structures are summarized in Table 1. Cys 115 lies out of allowed regions in the Ramachandran plot; the nucleophile elbow cysteine residue is a Ramachandran outlier in all proteins of known structure in the DJ-1 superfamily. Residue 55 lies at the edge between nonallowed and generously allowed regions of the plot. However, the electron density is well-defined for this residue. The main chain conformation of Asp 55 is stabilized by the interactions of the backbone amide hydrogen with one of the side chain oxygens of Glu 21, and of the carbonyl oxygen with a water molecule (water molecule 23 in monomer A and water molecule 50 in monomer B). Examination of the electron density maps suggested that residue 136 was a serine instead of a proline (from sequence). The serine side chain fits the map well, whereas a proline cannot be correctly positioned in this region; crystallographic refinement leads to puckering amplitudes that are outside the normal range, and unacceptable main chain distortions. For this reason, residue 136 was modeled as a serine rather than a proline in our structure. Figures 2−4 were prepared using PyMOL (*34*).

The atomic coordinates and measured structure factors amplitudes of DR1199 have been deposited in the Protein Data Bank as entry 2vrn.

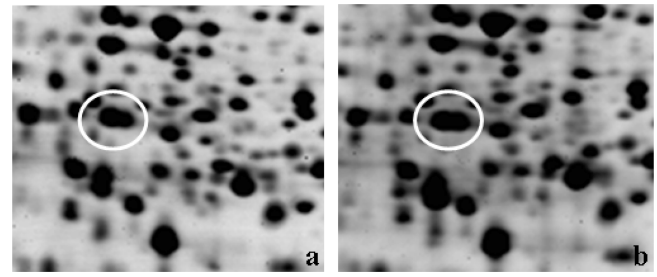

FIGURE 1: Close-up of DR1199 on a 2D PAGE gel. (a) Control sample from nonirradiated cells of *D. radiodurans*. (b) Sample from cells irradiated with a 5000 Gy X-ray dose (recovery time of 3 h). The expression level increases of more than 3 times upon irradiation.

Biochemical Characterization. Samples of the protein preparation used for crystallization, with and without the addition of peroxide, were used to determine the oligomeric state of the protein, under both reducing and oxidizing conditions. Mass spectrometry analysis was performed on the same samples to determine the oxidation state of the protein and verify if the modification on Cys 115 was already present before crystallization. The protein was also tested for proteolytic and chaperone activity.

Oligomerization State Analysis. (i) Size-Exclusion Chromatography. Protein samples with and without 5 mM H_2O_2 were incubated at 4 °C overnight. Then 25 μL of each sample, containing 170 μg of protein, was applied to a Superose 12 10/300 GL column (Amersham Biosciences) previously equilibrated with 20 mM Tris-HCl and 150 mM NaCl (pH 7.5). The column was run with the same buffer at 0.8 mL/min in an Akta Purifier system (Amersham Biosciences).

(ii) Dynamic Light Scattering (DLS). The size distribution of DR1199 under reducing and oxidizing conditions was also measured by DLS in a Malvern Zetasizer Nano System. The samples were centrifuged for 10 min at 12000 rpm, and the supernatant was collected and used for the experiments in a 50 μL quartz cuvette. The analysis was performed on the samples (with and without the addition of a final concentration of 5 mM H_2O_2) before (0.4 mg/mL) and after (0.1 mg/mL) size-exclusion chromatography. All measurements were performed at 4 °C, and data were recorded over 100 s.

(iii) Sucrose Gradient. Linear density gradients were prepared from 10 to 30% (w/w) sucrose in buffer SG [20 mM Tris-HCl, 150 mM NaCl, and 0.5 mM EDTA (pH 7.5)]. The 11 mL gradients were made in Ultra-Clear centrifuge tubes (Beckman) using a Hoefer SG 15 two-chamber gradient maker (Amersham Biosciences) and were poured using a peristaltic pump. Protein samples of 500 μL, containing 0.2 mg of protein in buffer SG, were applied to the top of the 10 to 30% sucrose gradients and centrifuged for 20 h in a Beckman L-80 ultracentrifuge at 35000 rpm and 4 °C in a SW41Ti rotor. Gradient solutions and protein samples were added with H_2O_2 up to a final concentration of 5 mM when checking the protein oligomeric state under oxidizing conditions. The gradients were calibrated using the following standard proteins (Amersham Biosciences): thyroglobulin (703 kDa), catalase (240 kDa), and albumin (67.4 kDa). Gradient fractionation was carried out bottom-up using a capillary tube connected to a peristaltic pump. The pump was coupled to the lamp inlet of an Akta Prime system (Amersham Biosciences), and the chromatographic system

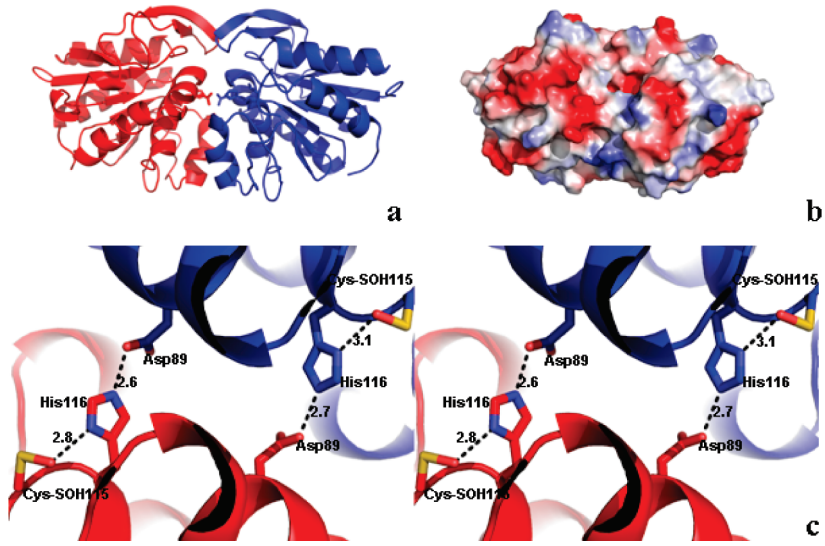

FIGURE 2: Overall structure of the functional DR1199 dimer. (a) Protein, shown in ribbon representation (monomer A colored red, monomer B colored blue), displaying a dimer interface similar to that observed with the YhbO and *Ph*pI proteins. (b) Electrostatic potential. Formation of the dimer buries ~1000 Å^2 of solvent-accessible surface. (c) Stereo picture of the DR1199 putative active sites. Secondary structures are shown as ribbons and side chains of residues in the triad as sticks. Two triads form at the interface between monomers. Two residues belong to one monomer [Cys 115, modeled as sulfenic acid (Cys-SOH) and His 116], and one belongs to the other (Asp 89). The hydrogen bonds between side chains in the triad are shown as dotted lines.

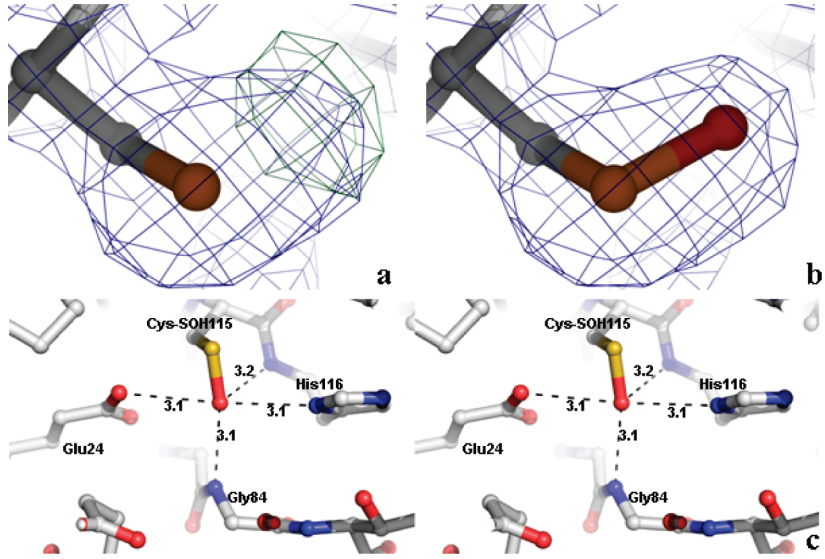

FIGURE 3: Cysteinesulfenic acid at position 115 in the crystal structure of DR1199. (a and b) The $2mF_O - DF_C$ electron density (blue; contoured at 1.0σ) and $mF_O - DF_C$ electron density (red, negative; green, positive; contoured at ±4 σ, m and D are weights for the Fourier coefficients). Electron density maps were calculated before the introduction of the oxygen atom of Cys-SOH 115 in panel a and afterward in panel b. A significant positive peak is observed next to the sulfur atom of Cys 115 in panel a; this peak disappears when modeled as the oxygen of a cysteine modified to sulfenic acid in panel b. (c) Stereo picture of the environment of Cys-SOH 115, showing all atoms within 6 Å. Dotted lines represent hydrogen bonds between Cys-SOH 115 and the surrounding residues, Glu 24, His 116, and Gly 84.

was run at the same flow rate (0.5 mL/min) as the peristaltic pump to produce continuous absorbance at 280 nm and conductivity data. Fractions of 0.6 mL were collected, and the presence of DR1199 was analyzed by SDS−PAGE. For this, an aliquot of each fraction was mixed 1:1 with 50 mM Tris buffer (pH 6.8) containing 8 M urea, 2 M thiourea, 75 mM DTT, 3% (w/v) SDS, and 0.05% bromophenol blue. The mixtures were heated at 100 °C for 4 min, and 15 μL of each was used for electrophoresis. SDS−PAGE gels (12%) were prepared and stained with Coomassie brilliant blue R-250 (*35*). Standard proteins from Fermentas were run simultaneously.

Proteolytic Activity. Proteolysis of fluorescein-isothiocyanate-conjugated casein (FITC-casein type III, Sigma) was assayed by incubation of the reaction mixtures containing 100 μg/mL substrate and 1 or 10 μg/mL DR1199 at 37 °C in 50 mM Tris-HCl (pH 8). The series were repeated in the presence of 1 mM $ZnCl_2$ and/or 1 mM DTT. Aliquots of the reaction mixtures were taken at different times, and the reaction was stopped by 1:1.5 dilution in 0.5 N TCA. Precipitated protein was removed by centrifugation, and 120 μL of supernatant was added to 180 μL of 0.2 M sodium phosphate (pH 8) directly in the wells of a 96-well plate. Fluorescence produced by FITC-labeled peptides was measured in a VICTOR 1420 multilabel counter (Wallac) using excitation and emission wavelengths of 485 and 535 nm, respectively. Chymotrypsin (sequencing grade, Roche) was used as a positive control.

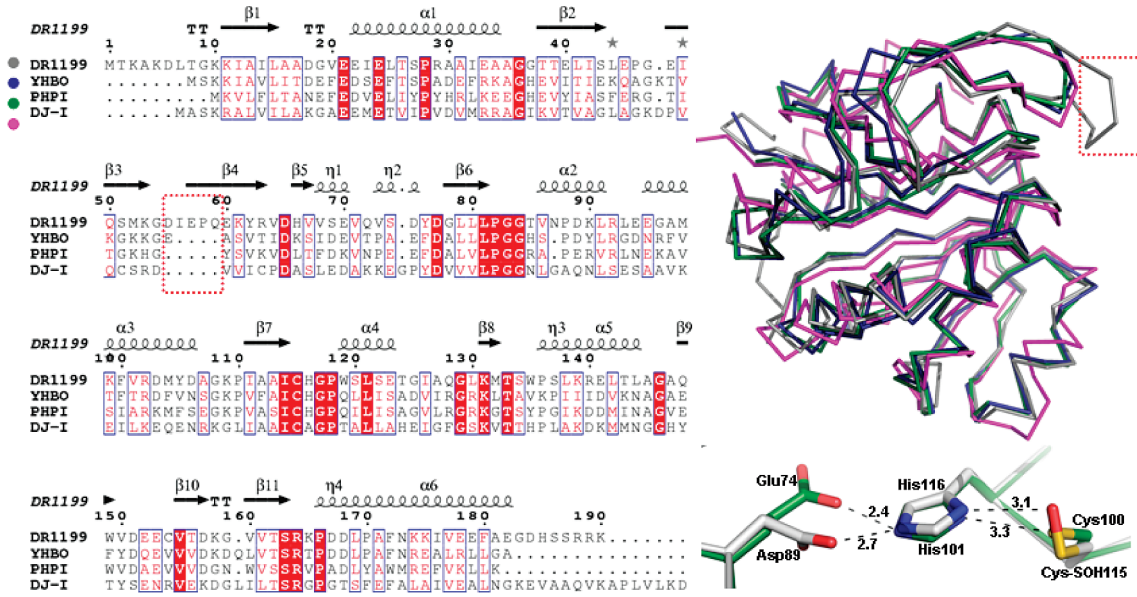

FIGURE 4: Comparison of DR1199 to other members of the DJ-1/ThiJ/*Pf*pI superfamily. The left panel shows a sequence alignment of DR1199 with the YhbO (38% sequence identity), *Ph*pI (37% sequence identity), and DJ-1 (24% sequence identity) proteins. Identical residues are colored white on a red background and similar residues red on a white background. For the secondary structure assignment, α-helices are represented as helices, *β*-strands are represented as arrows, and *β*-turns are marked with TT. An insertion of five residues is observed for the DR1199 sequence between residues 55 and 59 (dotted red line). This panel was prepared with ESPript (*46*). The right panel shows the superposition of DR1199 (gray) with the structures of YhbO (blue, 0.9 Å rmsd, PDB entry 1OI4), *Ph*pI (green, 0.9 Å rmsd, PDB entry 1G2I), and DJ-1 (magenta, 1.5 Å rmsd, PDB entry 1SOA). The major difference between DR1199 and the other structures is represented by the loop between residues 55 and 59 (dotted red line). A superposition of the putative active site of DR1199 (gray) and *Ph*pI (green) is also shown. The triads superimpose well, although a different orientation is observed for the side chains of Glu 74 and Asp 89, which results in a longer hydrogen bond between the imidazole ring and the carboxylic group in the case of DR1199.

Endopeptidase and aminopeptidase activities were assayed by monitoring the production of 7-aminomethylcoumarin (AMC) or *p*-nitroaniline (pNA) from the substrates: Ala-pNA, Arg-pNA, Lys-pNA, His-pNA, Gly-pNA, Phe-pNA, Tyr-AMC, succinyl-Ala-Ala-pNA, succinyl-Leu-Tyr-AMC, succinyl-Ala-Ala-Phe-AMC, carbobenzyloxy-Gly-Gly-Arg-AMC, and succinyl-Leu-Leu-Val-Tyr-AMC. Reactions were initiated by addition of DR1199 (1 or 10 μg/mL) to a prewarmed mixture containing the chromogenic (5 mM) or fluorogenic (0.5 mM) compound in 50 mM Tris-HCl (pH 8.0) at 37 °C. The series were repeated in the presence of 1 mM $ZnCl_2$ or 1 mM DTT. Aliquots of the reaction mixtures were taken at different times, and the reaction was stopped by 1:1 dilution in 0.1 M acetic acid. The quantity of pNA or AMC liberated was measured in a VICTOR 1420 multilabel counter (Wallac). For pNA, absorbance was determined at 405 nm, and for AMC, fluorescence was measured using excitation and emission wavelengths of 355 and 460 nm, respectively. Appropriate blanks without DR1199 were assayed for each experimental point.

Chaperone Activity. (i) Citrate Synthase Aggregation Suppression Assay. For thermal aggregation experiments, 0.4 μM (final concentration) bovine heart citrate synthase (CS, Sigma) was incubated at 45 °C in prewarmed 40 mM HEPES (pH 7.8), 20 mM KOH, 50 mM KCl, 10 mM NH_4SO_4, and 2 mM NH_3COOK. DR1199 was added to the reaction buffer at different molar excess ratios (from 1:1 to 20:1). BSA (Sigma) at a 6-fold molar excess over CS was substituted for DR1199 in control experiments. CS aggregation was monitored in the thermostated cell of an Aminco fluorescence spectrophotometer. Right angle light scattering was recorded with excitation and emission wavelengths set at 500 nm. The same experiments were also performed on DR1199 (final concentration of 2 mM) incubated overnight at 4 °C with 8 mM H_2O_2.

(ii) Citrate Synthase Reactivation Assay. For the thermal reactivation assay, 0.4 μM CS was incubated in 150 mM Tris (pH 8) in the presence of a molar excess of DR1199 (up to 20:1). Samples were incubated at 45 °C for 30 min for enzyme denaturation and cooled to 23 °C for renaturation. The recovered CS activity was assayed after 1 h as described previously (*36*) and compared to that of samples maintained at 23 °C. The same experiments were also performed on DR1199 (final concentration of 2 mM) incubated overnight at 4 °C with 8 mM H_2O_2.

Electrospray Mass Spectrometry. Protein samples were first diluted in a 0.2% formic acid solution to produce a 2 μM solution of protein; 2 μL was loaded on a protein MicroTrap (Michrom Biosresources, Auburn, CA), desalted for 5 min with a 0.2% formic acid solution, and then loaded and eluted on a Poroshell 300SB-C8 column (Agilent Technologies). Mass spectral analysis was performed on a Q-TOF Micro instrument (Micromass, Manchester, U.K.) operating with a needle voltage of 3000 V and with sample and extraction cone voltages of 60 and 0.2 V, respectively. Mass spectra were recorded in the 500−1600 mass-to-charge (*m*/*z*) range. Mass spectra were acquired and the data processed with MassLinx 4.0 (Waters).

Maldi-TOF Analysis. Protein samples were digested for 18 h at room temperature with endoproteinase Lys-C at a DR1199:Lys-C ratio of 10:1. Lysates were diluted into the matrix solvent (50:50:0.2 water/acetonitrile/formic acid) to a final concentration of 0.5 μM. Samples (0.5 μL) of this final preparation were dried with 0.5 μL of matrix solution (α-cyano-4-hydroxycinnamic acid), and Maldi-Tof mass

spectra were recorded on an Autoflex (Bruker, Bremen, Germany) mass spectrometer in reflection mode.

RESULTS

Overexpression after Irradiation. Computer-assisted comparative analysis of 2D PAGE gel protein patterns of nonirradiated and irradiated *D. radiodurans* cells revealed 13 proteins exhibiting a significant change in expression level upon irradiation. All these differentially expressed proteins were submitted to MS analysis for identification. In particular, the expression level of DR1199 shows a 3-fold increase after exposure of *D. radiodurans* cells to a dose of 5000 Gy of synchrotron radiation (Figure 1).

Structure Description. DR1199 was found to exist as a dimer both in solution and in the crystal form. The protein monomer has the characteristic flavodoxin-like fold (A domain) common to all the members of the DJ-1/ThiJ/*Pf*pI superfamily. Proteins of the DJ-1 superfamily function as oligomers, with variable oligomeric state and oligomerization interfaces. DR1199 displays a dimer interface similar to that observed for *Ph*pI and YhbO (Figure 2a), with the putative active sites forming at the interface.

The sequence alignment and structure superposition show that DR1199 shares characteristics with members of the DJ-1 family belonging to three different kingdoms of life: 38% sequence identity and 0.9 Å rmsd with respect to the bacterial YhbO, 37% sequence identity and 0.9 Å rmsd with respect to the archaeal *Ph*pI, and 24% sequence identity and 1.5 Å rmsd with respect to human DJ-1 (Figure 4). The most striking difference between DR1199 and its homologous proteins from the DJ-1 superfamily is represented by a loop located between residues 55 and 59. This loop is much longer in DR1199 than in the other structures (Figure 4). When an attempt to reconstruct a putative hexameric complex of DR1199 was made by superposition to the *Ph*pI hexameric structure (PDB entry 1G2I), the 55−59 loops protrude toward the center of the ring and clash with other molecules (not shown), preventing the formation of higher-order molecules.

Like the other members of the DJ-1 family, DR1199 contains the nucleophile elbow domain (*19*), consisting of a sharp turn between a β-strand and an α-helix and characterized by an unusually strained backbone conformation. The absolutely conserved cysteine lies in this region. In the YhbO protein, Cys 104 is required for *E. coli* stress resistance (*15*). The same residue is essential for the protease activity of some members of the family and may also be involved in other types of enzymatic activity. Cys 115 in DR1199 forms a triad with His 116 from the same monomer and Asp 89 of the other monomer in the dimer. As a result, two active sites are formed at the interface between the two monomers (Figure 2c).

The nucleophile elbow cysteine residue has been shown to be sensitive to oxidative modifications in the DJ-1 Parkinson's disease protein and in its close homologues YDR533Cp from *Saccharomyces cerevisiae* and YajL from *E. coli*. The crystal structures show that this residue is oxidized to a cysteinesulfenic (Cys-SOH) or cysteinesulfinic (Cys-SO_2H) acid in YajL (*16*), to cysteinesulfinic or -sulfonic (Cys-SO_3H) acid in DJ-1 (*37, 38*), and to a mixture of oxidized forms in YDR533Cp (*39*). DR1199 also exhibits modification at this residue, and the electron density in this region indicates that Cys 115 is oxidized to sulfenic acid (Figure 3a,b) in both monomers in the crystal. The oxygen atom in Cys 115-sulfenic acid is stabilized by its interactions with the carboxylic oxygen of Glu 24, the π-nitrogen of His 116, and the backbone amide hydrogen atoms of Gly 84 and His 116 (Figure 3c). The DR1199 sequence contains two cysteine residues (115 and 154), but only the cysteine in the nucleophile elbow is observed to be oxidized in the crystal structure.

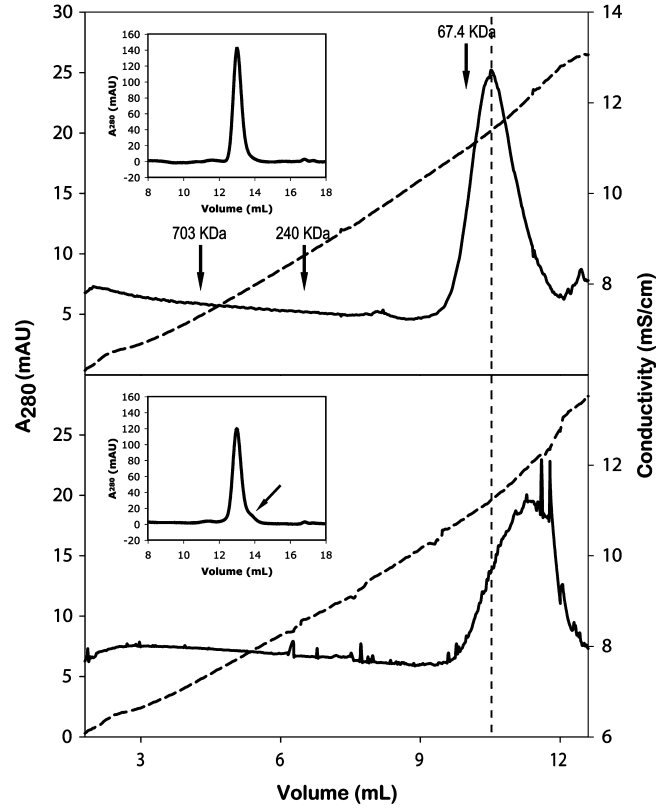

FIGURE 5: Analysis of the oligomerization state of DR1199 by size-exclusion chromatography and sucrose density gradient ultracentrifugation in the presence (bottom) or absence (top) of H_2O_2. This figure represents the absorbance at 280 nm (—) and the conductivity (– – –) as a function of the gradient volume. The insets show the chromatograms from size-exclusion analysis. The protein is in its dimeric state. In the presence or absence of H_2O_2, no higher-macromolecular weight complexes were observed. However, under oxidizing conditions, the chromatogram from size exclusion shows a tail to a lower molecular weight for the main peak; also, in the sucrose gradient, the peak maximum is displaced toward lower-molecular weight positions with respect to the untreated sample. These results suggest that a small fraction of the dimer may decompose to the monomer under oxidizing conditions.

Biochemical Characterization. Samples of DR1199 under reducing and oxidizing conditions were analyzed to determine the oligomerization state of the protein by size-exclusion chromatography, dynamic light scattering, and ultracentrifugation in sucrose density gradient. The protein was always observed to be in its dimeric state. In the presence or absence of H_2O_2, no higher-macromolecular weight complexes were observed for any of the samples (Figure 5). However, careful observation of the results obtained from the sucrose gradient suggests that the DR1199 dimer may not be completely resistant to peroxide. When H_2O_2 is present, the protein peak in the sucrose density gradient is broadened and its maximum is displaced toward lower-molecular weight positions with respect to the untreated

sample (Figure 5), indicating that a partial destabilization of the dimer to monomer may occur under oxidizing conditions.

DR1199 was tested for proteolytic activity. We could not detect proteolytic activity toward FITC-casein or any of the peptidase substrates that were tested (see Materials and Methods), even when high protein:substrate ratios and long incubation times (more than 3 h) were used. Negative results were also obtained in the presence of DTT and/or $ZnCl_2$ under conditions similar to those used to assay *E. coli* Hsp31 peptidase activity (*40*). Taking into account the fact that these or similar compounds have been found to be substrates of *Pf*pI (*21, 41*) or *E. coli* Hsp31 (*40*), our results suggest that the peptidase activity of DR1199, if present, is very low and therefore the protein does not function mainly as a protease. Negative results were also obtained when DR1199 molecular chaperone-like activity was tested for the refolding and reactivation of citrate synthase under both reducing and oxidizing conditions.

To determine whether oxidation at Cys 115 occurs prior or subsequent to crystallization, we analyzed the DR1199 preparation by mass spectrometry. Identification of the types and the sites of oxidative modifications is dependent on the ability to generate peptide fragments of appropriate size that ideally should cover the entire length of the amino acid sequence. For this purpose, the protein preparation used for crystallization was digested with the protease Lys-C and analyzed by mass spectrometry. Peptides containing Cys 115 were recovered and showed the residue being in its reduced state. The same protein preparation, treated with H_2O_2, was also digested and analyzed by mass spectrometry. Unfortunately, no peptides containing Cys 115 could be recovered from the samples treated with peroxide. These results suggest that oxidation of the conserved cysteine to sulfenic acid is subsequent to crystallization; however, we could not determine the direct effect of peroxide on Cys 115 in solution.

The mass of the undigested protein was also determined by mass spectrometry analysis, and a difference of 16 Da was found between the two samples (with or without H_2O_2). These results strongly suggest that a mild treatment with peroxide oxidizes Cys 115 to sulfenic acid in solution. The crystals took ~2 months to grow; during this period, oxidation might have been promoted by the presence of trace amounts of metal ions in the crystallization solution or by peroxide decomposition products in the polyethylene glycol used as a precipitant for crystal growth (*37*).

DISCUSSION

In the crystal structure, DR1199 is observed in its dimeric state, and other biophysical tests indicate that the formation of higher-order molecular complexes is not likely to be an important part of the biological function of this protein. In addition, no proteolytic activity was detected, suggesting that DR1199 performs some as yet unknown biological function.

The archaeal homologous of DR1199, *Pf*pI and *Ph*pI, have been identified as ATP-independent peptidases (*21, 22*). *Pf*p1 is suggested to be a processive type of protease with broad specificity, as in the archaeal and the eukaryotic proteasome (*41, 21*). In vitro proteolytically active trimeric, hexameric, and higher trimer-based forms are observed, whereas the monomer is inactive. Similarly, *Ph*pI has been proposed to work as a hexamer (although dimers and trimers also exhibit proteolytic activity) where access to the active sites is restricted by a small opening.

When DR1199 is compared to *Ph*pI, a longer loop due to an insertion in the amino acid sequence is observed between residues 55 and 59 for the bacterial protein (Figure 4). In any putative DR1199 hexamer, these loops from different monomers would point toward the center of the ring and clash with each other, destabilizing the formation of such a complex. In *Ph*pI, the active sites are located in hindered positions in the hexameric ring, not accessible to the smallest globular protein, to prevent the indiscriminate digestion of cytoplasmic proteins (*22*). In DR1199, we do not observe such compartmentalization; this observation alone suggests that the regulation of the protein activity or even its function may be different from that observed in *Ph*pI.

In our structure, Cys 115 is oxidized to sulfenic acid. The modification was not intentionally produced and occurred spontaneously in the crystallization solution through a reaction that has been demonstrated to be reversible in proteins (*42*). The reversible oxidation of this cysteine could not only provide a means for DR1199 to sense the stress but also a way to control the activity of the protein in the cell.

Although size-exclusion chromatography and dynamic light scattering suggest DR1199 to be mostly in its dimeric state under reducing and oxidizing conditions, sucrose gradient separation by ultracentrifugation reveals the possibility of partial destabilization of the dimer to monomer upon oxidation (Figure 5). In DR1199, the dimer formation buries ~1000 $Å^2$ of solvent-accessible surface and the putative active sites form at this interface with two residues given by one monomer and one by the other. The separation of the monomers would therefore disrupt the triads.

The Parkinson's disease protein DJ-1 and other two members of the DJ-I superfamily, YDR533Cp from *S. cerevisiae* and YajL from *E. coli*, have also been found to be readily oxidized on the conserved cysteine residue located in the nucleophile elbow. The function of YDR533Cp and YajL is unknown, whereas in the case of DJ-1, the oxidation state is proposed to regulate its chaperone activity toward α-synuclein (*43*). DJ-1 is also able to eliminate H_2O_2 in vitro by autoxidation, acting as a scavenger on peroxide; for this reason, it has been proposed to have a role in the protection against oxidative stress and prevention of cell death (*44*). We could not detect any proteolytic or chaperone activity for DR1199; therefore, its function is still unknown but is certainly involved in the response to stress. Similar to DJ-I, DR1199 may play a role in the protection of the cell from oxidation. Overexpressed after irradiation, DR1199 is available in large quantities to the bacterium, as observed for many proteins involved in the detoxification of *D. radiodurans* cells. By spontaneous and rapid oxidation of its highly reactive cysteine, DR1199 would be able to scavenge peroxide molecules or other dangerous reactive oxygen species produced by irradiation, limiting the oxidative damage to DNA and other proteins. It is also possible that the acidic isoform of the protein would accumulate under these conditions because of the presence of reactive oxygen species; in particular, *D. radiodurans* cells were found to release H_2O_2 during irradiation (*5*).

A recent study on a YhbO-deficient strain bacteria (*15*) has identified YhbO as a general stress protein involved in protecting the cell from UV irradiation and other stresses such as oxidation, heat, and extreme pH. The conserved cysteine appears to be indispensable for the function of YhbO. DR1199 and YhbO are very similar in sequence, structure organization, and oligomerization. Both proteins have an Asp in the putative triad (where *Ph*pI and *Pf*pI have a Glu), do not form high-molecular weight complexes, and lack proteolytic activity (*45*). These observations agree with our suggestion that DR1199 is not a protease and most probably, as in the case of YhbO, is a stress response protein whose exact function has yet to be characterized.

ACKNOWLEDGMENT

We thank Lauriane Kuhn and Jerome Garin (Laboratoire de chimie des protéines CEA, Grenoble, France) for the identification of DR1199 from the 2D gels.

SUPPORTING INFORMATION AVAILABLE

Mass spectrograms of oxidized and reduced DR119 prepared as described in Materials and Methods, where a difference of 16 Da was found between the two samples (with or without H_2O_2). This material is available free of charge via the Internet at http://pubs.acs.org.

REFERENCES

1. Cox, M. M., and Battista, J. R. (2005) *Deinococcus radiodurans*: The consummate survivor. *Nat. Rev. Microbiol. 3*, 882–892.
2. Levin-Zaidman, S., Englander, J., Shimoni, E., Sharma, A. K., Minton, K. W., and Minsky, A. (2003) Ringlike structure of the *Deinococcus radiodurans* genome: A key to Radioresistance? *Science 299*, 254–256.
3. Battista, J. R., Earl, A. M., and Park, M. J. (1999) Why is *Deinococcus radiodurans* so resistant to ionizing radiation? *Trends Microbiol. 7*, 362–365.
4. Daly, M. J., Gaidamakova, E. K., Matrosova, V. Y., Vasilenko, A., Zhai, M., Venkateswaran, A., Hess, M., Omelchenko, M. V., Kostandarithes, H. M., Makarova, K. S., Wackett, L. P., Fredrickson, J. K., and Ghosal, D. (2004) Accumulation of Mn(II) in *Deinococcus radiodurans* facilitates gamma-radiation resistance. *Science 306*, 1025–1028.
5. Daly, M. J., Gaidamakova, E. K., Matrosova, V. Y., Vasilenko, A., Zhai, M., Leapman, R. D., Lai, B., Ravel, B., Li, S. M., Kemner, K. M., and Fredrickson, J. K. (2007) Protein oxidation implicated as the primary determinant of bacterial radioresistance. *PLoS Biol. 5* (4), e92.
6. Karlin, S., and Mrázek, J. (2001) Predicted highly expressed and putative alien genes of *Deinococcus radiodurans* and implications for resistance to ionizing radiation damage. *Proc. Natl. Acad. Sci. U.S.A. 98*, 5240–5245.
7. Zhang, C., Wei, J., Zheng, Z., Ying, N., Sheng, D., and Hua, Y. (2005) Proteomic analysis of *Deinococcus radiodurans* recovering from γ-irradiation. *Proteomics 5*, 138–143.
8. Makarova, K. S., Aravind, L., Wolf, Y. I., Tatusov, R. L., Minton, K. W., Koonin, E. V., and Daly, M. J. (2001) Genome of the Extremely Radiation-Resistant Bacterium *Deinococcus radiodurans* Viewed from the Perspective of Comparative Genomics. *Microbiol. Mol. Biol. Rev. 65*, 44–79.
9. Airo, A., Chan, S. L., Martinez, Z., Platt, M. O., and Trent, J. D. (2004) Heat shock and cold shock in *Deinococcus radiodurans*. *Cell Biochem. Biophys. 40*, 277–288.
10. Bonifati, V., Rizzu, P., van Baren, M. J., Schaap, O., Breedveld, G. J., Krieger, E., Dekker, M. C., Squitieri, F., Ibanez, P., Joosse, M., van Dongen, J. W., Vanacore, N., van Swieten, J. C., Brice, A., Meco, G., van Duijn, C. M., Oostra, B. A., and Heutink, P. (2003) Mutations in the DJ-1 gene associated with autosomal recessive early-onset parkinsonism. *Science 299*, 256–259.
11. Sastry, M. S., Korotkov, K., Brodsky, Y., and Baneyx, F. (2002) Hsp31, the *Escherichia coli* yedU gene product, is a molecular chaperone whose activity is inhibited by ATP at high temperatures. *J. Biol. Chem. 277*, 46026–46034.
12. Mujacic, M., and Baneyx, F. (2007) Chaperone Hsp31 contributes to acid resistance in stationary-phase *Escherichia coli*. *Appl. Environ. Microbiol. 73*, 1014–1018.
13. Shendelman, S., Jonason, A., Martinat, C., Leete, T., and Abeliovich, A. (2004) DJ-1 is a redox-dependent molecular chaperone that inhibits α-synuclein aggregate formation. *PLoS Biol. 2* (11), e362.
14. Weber, A., Kogl, S. A., and Jung, K. (2006) Time-Dependent Proteome Alterations under Osmotic Stress during Aerobic and Anaerobic Growth in *Escherichia coli*. *J. Bacteriol. 188*, 7165–7175.
15. Abdallah, J., Caldas, T., Kthiri, F., Kern, R., and Richarme, G. (2007) YhbO Protects Cells against Multiple Stresses. *J. Bacteriol. 189*, 9140–9144.
16. Wilson, M. A., Ringe, D., and Petsko, G. A. (2005) The atomic resolution crystal structure of the YajL (ThiJ) protein from *Escherichia coli*: A close prokaryotic homologue of the Parkinsonism-associated protein DJ-1. *J. Mol. Biol. 353*, 678–691.
17. Wei, Y., Ringe, D., Wilson, M. A., and Ondrechen, M. J. (2007) Identification of functional subclasses in the DJ-1 superfamily proteins. *PLoS Comput. Biol. 3* (1), e10.
18. Chang, L. S., Hicks, P. M., and Kelly, R. M. (2001) Protease I from *Pyrococcus furiosus*. *Methods Enzymol. 330*, 403–413.
19. Ollis, D. L., Cheah, E., Cygler, M., Dijkstra, B., Frolow, F., Franken, S. M., Harel, M., Remington, S. J., Silman, I., Schrag, J., et al. (1992) The α/β-hydrolase fold. *Protein Eng. 5*, 197–211.
20. Quigley, P. M., Korotkov, K., Baneyx, F., and Hol, W. G. (2003) The 1.6-Å crystal structure of the class of chaperones represented by *Escherichia coli* Hsp31 reveals a putative catalytic triad. *Proc. Natl. Acad. Sci. U.S.A. 100*, 3137–3142.
21. Halio, S. B., Bauer, M. W., Mukund, S., Adams, M. W. W., and Kelly, R. M. (1997) Purification and Characterization of Two Functional Forms of Intracellular Protease PfpI from the Hyperthermophilic Archaeon *Pyrococcus furiosus*. *Appl. Environ. Microbiol. 63*, 289–295.
22. Du, X., Choi, I. G., Kim, R., Wang, W., Jancarik, J., Yokota, H., and Kim, S. H. (2000) Crystal structure of an intracellular protease from *Pyrococcus horikoshii* at 2-Å resolution. *Proc. Natl. Acad. Sci. U.S.A. 97*, 14079–14084.
23. Rawlings, N. D., Morton, F. R., and Barrett, A. J. (2006) MEROPS: The peptidase database. *Nucleic Acids Res. 34*, D270–D272.
24. Powell, H. R. (1999) The Rossmann Fourier autoindexing algorithm in MOSFLM. *Acta Crystallogr. D55*, 1690–1695.
25. Collaborative Computational Project, Number 4 (1994) The CCP4 Suite: Programs for Protein Crystallography. *Acta Crystallogr. D50*, 760–763.
26. Read, R. J. (2001) Pushing the boundaries of molecular replacement with maximum likelihood. *Acta Crystallogr. D57*, 1373–1382.
27. Perrakis, A., Morris, R., and Lamzin, V. S. (1999) Automated protein model building combined with iterative structure refinement. *Nat. Struct. Biol. 6*, 458–463.
28. Emsley, P., and Cowtan, K. (2004) Coot: Model-building tools for molecular graphics. *Acta Crystallogr. D60*, 2126–2132.
29. Murshudov, G. N., Vagin, A. A., and Dodson, E. J. (1997) Refinement of macromolecular structures by the maximum-likelihood method. *Acta Crystallogr. D53*, 40–55.
30. Winn, M. D., Isupov, M. N., and Murshudov, G. N. (2001) Use of TLS parameters to model anisotropic displacements in macromolecular refinement. *Acta Crystallogr. D57*, 122–133.
31. Murshudov, G. N., Vagin, A. A., Lebedev, A., Wilson, K. S., and Dodson, E. J. (1999) Efficient anisotropic refinement of macromolecular structures using FFT. *Acta Crystallogr. D55*, 247–255.
32. Laskowski, R. A., MacArthur, M. W., Moss, D. S., and Thornton, J. M. (1993) PROCHECK: A program to check the stereochemical quality of protein structures. *J. Appl. Crystallogr. 26*, 283–291.
33. Vriend, G. (1990) WHAT IF: A molecular modeling and drug design program. *J. Mol. Graphics 8*, 52–56.
34. DeLano, W. (2003) The PyMOL molecular graphics system, DeLano Scientific LLC, San Carlos, CA.
35. Laemmli, U. K. (1970) Cleavage of structural proteins during the assembly of the head of bacteriophage T4. *Nature 227*, 680–685.
36. Srere, P. A. (1969) Citrate synthase. In *Methods in Enzymology* (Lowenstein, J. M., Ed.) Vol. 13, pp 1−11, Academic Press, London.
37. Canet-Aviles, R. M., Wilson, M. A., Miller, D. W., Ahmad, R., McLendon, C., Bandyopadhyay, S., Baptista, M. J., Ringe, D., Petsko, G. A., and Cookson, M. R. (2004) The Parkinson's disease

protein DJ-1 is neuroprotective due to cysteine-sulfinic acid-driven mitochondrial localization. *Proc. Natl. Acad. Sci. U.S.A. 101*, 9103–9108.

38. Kinumi, T., Kimata, J., Taira, T., Ariga, H., and Niki, E. (2004) Cysteine-106 of DJ-1 is the most sensitive cysteine residue to hydrogen peroxide-mediated oxidation in vivo in human umbilical vein endothelial cells. *Biochem. Biophys. Res. Commun. 317*, 722–728.
39. Wilson, M. A., St Amour, C. V., Collins, J. L., Ringe, D., and Petsko, G. A. (2004) The 1.8-Å resolution crystal structure of YDR533Cp from *Saccharomyces cerevisiae*: A member of the DJ-1/ThiJ/PfpI superfamily. *Proc. Natl. Acad. Sci. U.S.A. 101*, 1531–1536.
40. Malki, A., Caldas, T., Abdallah, J., Kern, R., Eckey, V., Kim, S. J., Cha, S. S., Mori, H., and Richarme, G. (2005) Peptidase activity of the *Escherichia coli* Hsp31 chaperone. *J. Biol. Chem. 280*, 14420–14426.
41. Halio, S. B., Blumentals, I. I., Short, S. A., Merrill, B. M., and Kelly, R. M. (1996) Sequence, expression in *Escherichia coli*, and analysis of the gene encoding a novel intracellular protease (PfpI) from the hyperthermophilic archaeon *Pyrococcus furiosus*. *J. Bacteriol. 178*, 2605–2612.
42. Claiborne, A., Yeh, J. I., Mallett, T. C., Luba, J., Crane, E. J., Charrier, V., and Parsonage, D. (1999) Protein-sulfenic acids: Diverse roles for an unlikely player in enzyme catalysis and redox regulation. *Biochemistry 38*, 15407–15416.
43. Zhou, W., Zhu, M., Wilson, M. A., Petsko, G. A., and Fink, A. L. (2005) The Oxidation State of DJ-1 Regulates its Chaperone Activity Toward α-Synuclein. *J. Mol. Biol. 356*, 1036–1048.
44. Taira, T., Saito, Y., Niki, T., Iguchi-Ariga, S. M. M., Takahashi, K., and Ariga, H. (2004) DJ-1 has a role in antioxidative stress to prevent cell death. *EMBO Rep. 5*, 213–218.
45. Abdallah, J., Kern, R., Malki, A., Eckey, V., and Richarme, G. (2006) Cloning, expression, and purification of the general stress protein YhbO from *Escherichia coli*. *Protein Expression Purif. 47*, 455–460.
46. Gouet, P., Courcelle, E., Stuart, D. I., and Metoz, F. (1999) ESPript: Multiple sequence alignments in PostScript. *Bioinformatics 15*, 305–308.

BI800882V